

## INVESTIGATION ON THE WEAR BEHAVIOUR AND PROPERTIES OF RHA REINFORCED 7075 ALUMINIUM T6 COMPOSITES PRODUCED BY VACUUM INFILTRATION

Naci Arda Tanis<sup>1,\*</sup>, Onur Okur<sup>1</sup>, Che Nor Aiza Jafaar<sup>2,3</sup>, Azmah Hanim Mohamed Ariff<sup>2,3</sup> and Recep Çalin<sup>1</sup>

<sup>1</sup>Department of Metallurgy and Materials Engineering, Faculty of Engineering and Architecture, Kırıkkale University, 71450, Kırıkkale, Turkey

<sup>2</sup>Department of Mechanical and Manufacturing Engineering, Faculty of Engineering, Universiti Putra Malaysia, 43400 Serdang, Selangor, Malaysia

<sup>3</sup>Advanced Engineering Materials and Composites (AEMC), Department of Mechanical and Manufacturing Engineering, Faculty of Engineering, 43400 UPM Serdang, Selangor, Malaysia

\*ardatanis@kku.edu.tr

---

**Abstract.** Aluminum matrix composites containing hard ceramic particles have higher strength, hardness and wear resistance than conventional materials. However, the high cost of hard ceramic reinforcements has led researchers to obtain ceramic reinforcement from organic wastes such as rice husk and eggshell, and they are looking for ways to increase the hardness and wear properties by reinforced these organic wastes. In this study, 1, 2, and 4 vol.% rice husk ash (RHA) were added to AA7075 metal matrix. Samples were produced in a steel tube under 550 mmHg vacuum at 750 °C for 3 minutes. T6 heat treatment (aging) was applied to the samples. The density, porosity, and hardness of non-aged and aged samples were measured and compared. In addition, SEM and EDS analysis of aged samples were performed and wear properties under 20 N load was investigated. While the hardness and the porosity of T6 heat treated composites increased with increasing reinforcement volume ratio, T6 heat treatment did not improve the hardness and the wear properties of the composites significantly compared to unreinforced (0 vol%) sample. Wear tests showed that the mass loss increased with the increment of reinforcement-volume ratio. Increasing RHA content resulted in worsening the wear behavior of composites because of the poor wettability of RHA particles.

**Keywords:** Aluminium metal matrix composite, rice husk ash (RHA), heat treatment

---

### Article Info

Received 18<sup>th</sup> February 2022

Accepted 5<sup>th</sup> March 2022

Published 23<sup>rd</sup> December 2022

Copyright Malaysian Journal of Microscopy (2022). All rights reserved.

ISSN: 1823-7010, eISSN: 2600-7444

## Introduction

Aluminum metal matrix composites (AMCs) are frequently studied due to the prominent benefits such as improved strength in proportion to weight ratio, relatively low density, high thermal conductivity, better wear resistance, etc. [1]. Several techniques such as stir casting, vortex method, powder metallurgy, infiltration casting etc have been used to fabricate MMC product. It well known that infiltration method is widely used for making MMC with high volume fraction of reinforcement [2,3] The production of AMCs brings extra costs comparing to conventional aluminum alloys owing to multiple components and steps used in production [4]. The cost of AMCs can be lowered if agro-waste and its ceramic compounds are utilized as reinforcement particles [5]. The use of industrial agro-waste as reinforcement material has drawn remarkable attention in recent years due to the environmental awareness in our society [4,6-8]. Rice husk ash (RHA) is one of many industrial derivatives which is agricultural waste that has high availability worldwide. The great amount of harvesting paddy consists of rice, bran, and husk. This husk is used as fuel to provide energy in rice mills. During this process, husk is transformed into ash which is known as RHA. It is estimated that around 120 million tons of RHA was produced annually around the world. Therefore, the use of this agro-waste is of much interest among researchers in terms of environmental concerns [9-11].

Research on publication of RHA in AMC has been studied by many researchers [12,13] such as Ahamed et al. [13] produced RHA reinforced AMCs by using stir casting method. They found out that while density of composites decreased, tensile strength (TS) and hardness increased by increasing reinforcement ratio [12]. Alaneme et al. [13] studied the mechanical behavior of rice husk ash (RHA) and alumina reinforced aluminium hybrid composites produced by stir casting method. They reported that the hardness and TS of the hybrid composite was slightly lower when compared to single reinforced  $\text{Al}_2\text{O}_3/\text{Al}$  composites while the fracture toughness increased within percentage of RHA up to 3 wt%.

Prasad et al. [14] also used stir casting method to fabricate RHA/A356.2 metal matrix composites (MMCs). They stated that the hardness and ultimate tensile strength of the composites were higher when compared to pure alloy. In another study, Prasad et al. [15] produced A356.2 aluminium composite reinforced with rice husk ash (RHA) by stir casting method and its tribological properties were investigated. They reported that while the hardness of the composites increased with increasing rice husk ash content, the wear rate and friction coefficient of the composite decreased. Gladston et al. [16] studied on the production and wear properties of RHA reinforced AA6061 composites. Compo-casting method was chosen as production method and 0, 2, 4, 6, and 8 wt.% RHA reinforced composites were produced. It was found that RHA particles also refined the grain structure of aluminium and thus improved the wear resistance. The presence of RHA particles enhanced the wear resistance of composites and an increment in the applied load and the RHA particles switched the wear model [16].

Vacuum infiltration method used in metal matrix composites consists of following several steps: the melt and the reinforcement contact at the surface of particle preform, the infiltration starts with the melt flow through the preform under negative pressure and the solidification takes place [17,18]. Recently, hybrid techniques comprising of vacuum infiltration method were implemented to achieve improved mechanical properties [19,20].

Despite the fact that many new techniques have been developed in using RHA as reinforcing fillers in AMC to minimizing the amount of waste, application of vacuum infiltration method were missing in the literature although this method associated with this filler is one of the cost efficient, safe, fast, simple production processes compared to other production methods [21]. In this research, manufacturability of RHA reinforced aluminum composites using vacuum infiltration method was carried out and the wear behaviour and properties of RHA reinforced 7075 aluminium T6 composites was investigated.

## Materials and Methods

In this study, rice husk ash (RHA) particles (particle size: 125 to 250  $\mu\text{m}$ ) (supplied from Department of Mechanical and Manufacturing Engineering, Putra University, Malaysia) and AA7075 alloy were used. The chemical composition of the AA7075 alloy powder is 5.6 wt.% Zn, 2.6 wt.% Mg, 1.6 wt.% Cu, 2.6 wt.% Cr, and the rest is Al. The x-ray fluorescence (XRF) analysis was used to obtain the chemical composition of the RHA used in this study is 6.8 wt.% C, 56.4 wt.% O, 35.7 wt.% Si, 0.7 wt.% Ca, and 0.4 wt.% Mg. RHA was added to the matrix with the volume fractions of 1 %, 2 %, and 4 %.

Steel tubes with an outer diameter of 12 mm, wall thickness and height of 300 mm were used in the infiltration process as seen in Figure 1. Steel filters are placed at the bottom of the steel tubes to prevent powder from pouring. AA7075 and RHA powders were mixed with turbula 3D mixer to form the composite preforms having reinforcement volume fraction (R-V) of 1 %, 2 %, and 4 %. The mixed powders were placed into the steel pipes at a height of 70 mm. It is prevented from mixing with  $\text{SiO}_2$  powder by placing the filter mesh on the powder. After this process, the same height of  $\text{SiO}_2$  powders were placed on the top of mixed powders which prevented the melting metal from rising during the vacuum process. For melting the metal, an electrical resistance furnace was used. The melting furnace configuration were shown in Figure 1(b).

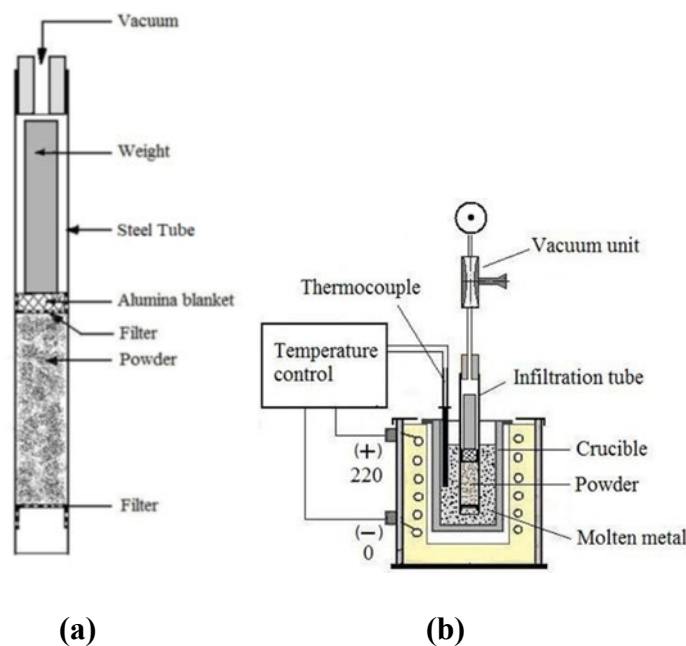


**Figure 1:** (a) Infiltration tube and (b) furnace used for manufacturing [21]

The melted aluminium alloy temperature was kept constant at  $750\text{ }^{\circ}\text{C} \pm 5$  throughout the experiment. About  $500 \pm 5$  mmHg vacuum pressure was applied to the tube and the steel tube was sunk into liquid aluminium. Vacuum was kept under these conditions for three minutes. After three minutes of vacuuming, the tubes were taken out and cooled down to room temperature in normal atmosphere. The tubes were carefully machined to remove the composites from the tubes. Non-infiltrated part was separated from infiltrated part as powder. Infiltration height and densities of composites were determined. The percentages of porosity of specimens have been determined in accordance with experimental and theoretical densities. Then, composites were cut into slices for microstructural examinations and heat treatment. The composites that were produced by vacuum infiltration were subjected to T6 heat treatment (aging) in order to increase the hardness of the composites by forming  $\text{MgZn}_2$  in the microstructure. Solution heat treatment was applied to the composites at  $485\text{ }^{\circ}\text{C}$  for two hours and then specimens were quenched. After that, composites were held in the heat treatment furnace at  $120\text{ }^{\circ}\text{C}$  for 24 hours.

The measurements of porosity, SEM and EDS analyzes of the aged samples were carried out by using JEOL JSM-6060LV and hardness measurements were performed using Galileo Durometria Vickers indenter with the loading force of 0.2 kg and a dwell time of 10 s. Thermogravimetry analysis-differential thermal analyses (TGA-DTA) analysis was performed to examine the thermal properties of RHA particles in molten metal at high temperature. After T6 heat treatment, XRD analysis were performed to determine the chemical composition of the intermetallic precipitates. Later, dry wear tests were carried out on the Pin-on disc device at a distance of 40 meters under 20 N load and with 240 mesh sandpaper.

## Results and Discussion

### *Density and Porosity Measurements*

Porosity (%) of the samples produced in the study were calculated based on Archimedes' method. Table 1 shows that the porosity increased in proportion to the increasing reinforcement ratio in non-aged samples. In this table, the actual density gives the ratio of actual weight to volume after infiltration and heat treatment.

**Table 1:** Density and porosity values of AMC produced

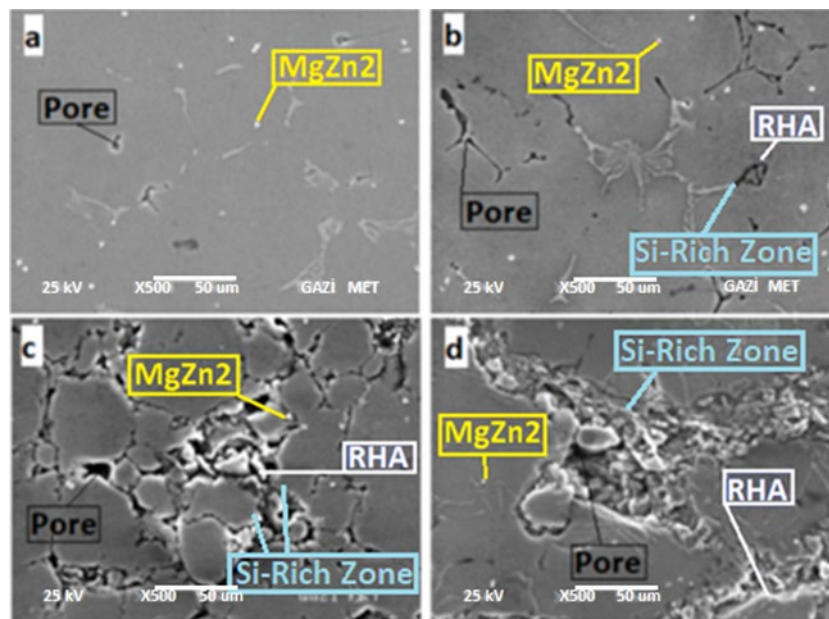
R-V fraction (vol%)	Non-aged			T6 Heat Treatment		
	True Density ( $\text{g/cm}^3$ )	Theoretical Density ( $\text{g/cm}^3$ )	Porosity (%)	True Density ( $\text{g/cm}^3$ )	Theoretical Density ( $\text{g/cm}^3$ )	Porosity (%)
0	2.733	2.811	2.774	2.602	2.811	6.688
1	2.683	2.804	4.315	2.458	2.804	13.358
2	2.569	2.798	8.184	2.625	2.798	11.924
4	2.415	2.787	13.347	2.401	2.787	13.254

After T6 heat treatment, it was observed that the porosity increased in the unreinforced sample (0 vol.%). The porosity increased drastically for the samples with 1 and 2 vol.% reinforcement ratios. It was determined that the increase in density of the sample was the highest at 4 vol% in the non-aged sample. The increase in the porosity after aging is due

to the expansion of the pores and diffusion of the matrix by the migration effect of Si and O atoms in the grain [22]. This mechanism may be explained with Kirkendall effect as reported by Zang et al. [23].

### Microstructure Analysis

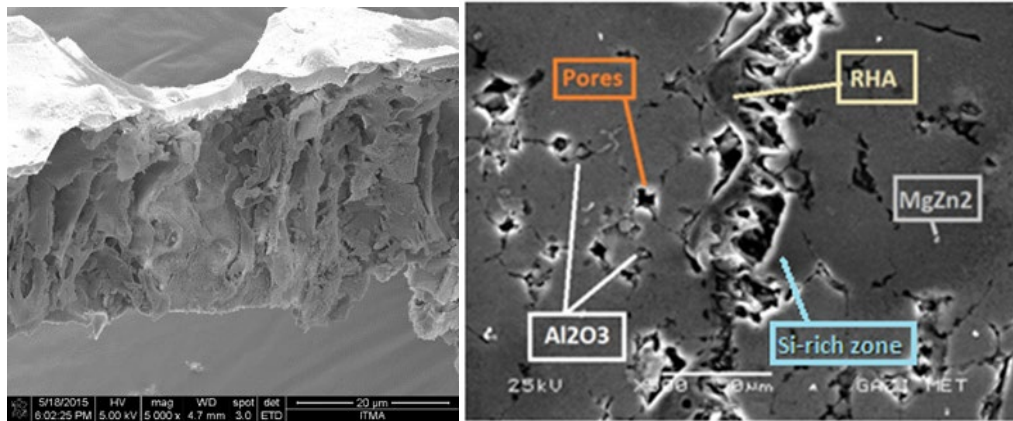
As can be seen from the SEM images of the produced samples (Figure 2), the non-reinforced sample seen in Figure 2(a) was less porous than the samples containing 1 and 2 vol% RHA reinforcement as shown in Figure 2(b) and (c), respectively. Figure 2 shows that the porosity (%) increased in proportion to the reinforcement rate in homogeneously distributed samples. The increase in porosity (%) is clearly seen in Table 1. The reason for this is that the RHA particles were formed due to their very porous structure as shown in Figure 2(a).



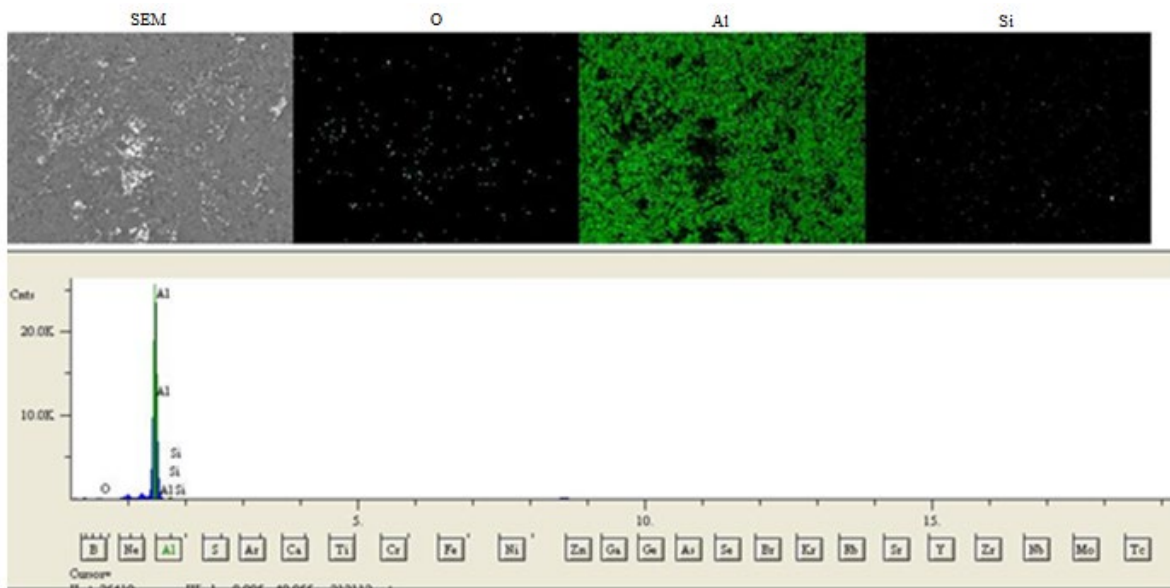
**Figure 2:** SEM images of RHA reinforced AA7075 matrix composite materials (a) non-reinforced alloy reinforced with (b) 1 vol% RHA, (c) 2 vol% RHA and (d) 4 vol% RHA.

Figure 3(a) shows the SEM images of the RHA particles, taken prior to its addition into the aluminum matrix. It was observed that the RHA particles were highly porous. From SEM images taken after production, it was seen that the large porosities appeared in the reinforced composites which were correspond to the RHA particles. (Figures 3(a) and (b)).

In the EDS analysis taken from the same region in which SEM images were taken, the high Si and O ratio in the large pores found in the matrix shows that SiO<sub>2</sub> compound was present in these pores. However, by dissolving the organic compounds left in the RHA at high temperature, the RHA component disintegrates in some regions over the matrix. In order to determine this situation, the EDS Mapping analysis with the results of the porous surface is shown Figure 4.



**Figure 3:** SEM images of (a) RHA and (b) the sample of 1 vol% reinforced RHA



**Figure 4:** EDS mapping analysis of the matrix sample reinforced with 2 vol% RHA of AA7075

In the EDS mapping analysis of the sample containing 2 % RHA reinforcement as shown in Figure 4, the green color represents the Al element, the blue colour represents the O element and the red element represent Si. As seen in SEM image, O and Si atoms in blue and red colour are distributed homogeneously in aluminium matrix and generally seen in same regions together. The fact that the results of the analyses were close to each other indicate that the  $\text{SiO}_2$  compound, the main compound of RHA, where found in these regions. In addition, in some regions where there is no O element, Si elements were found. These areas are located near the porous areas. The reason for the existence of Si element in the matrix close to the pores is the diffusion of Si into the Al matrix from RHA. Kumar et al. obtained similar results in their study on carbon nanotube reinforced aluminum composites [24].

## XRD Analyzes

The XRD spectrum of the sample without RHA reinforcement which was not subjected to heat treatment is given in Figure 5. It was determined that only  $\alpha$ -aluminum gave peaks as a result of analysis. No peaks were observed with regards the compounds of intermetallic or ceramic structure. When the XRD spectrum of the T6 heat treated and 1 wt.% RHA sample given in Figure 6 was examined, the peaks of  $MgZn_2$  intermetallic precipitates expected to appear after the heat treatment can be clearly seen.

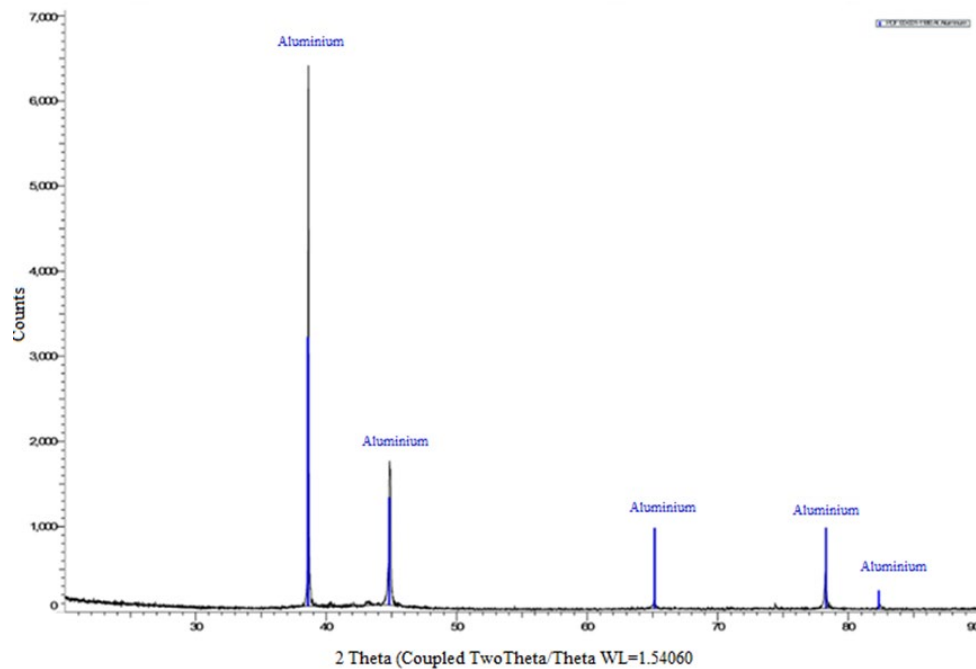


**Figure 5:** XRD spectrum of the Al alloy that not been heat treated and no reinforcements

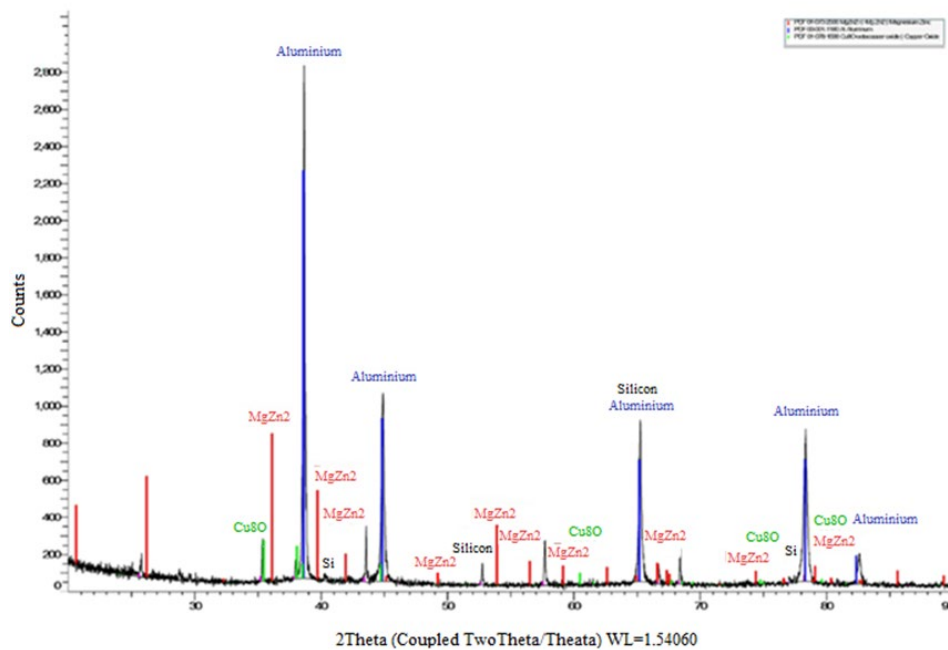


**Figure 6:** XRD spectrum of 1% RHA reinforced, AA 7075 matrix composite sample after T6 heat treatment



In addition, it was seen that the peaks of Si element occur in the regions where silicon passed into the matrix by diffusion around the RHA grain which was shown in Figure 2. Cu in the alloy resulted in the formation of  $\text{Cu}_2\text{O}$  compounds during heat treatment due to its high oxygen affinity.

### TGA-DTA Analysis

Figure 7 shows the TGA and DTA analyses of the reinforcement element. It was observed that the mass loss was 2.75 % in the samples when the temperature increased up to 700 °C. The loss of mass in the sample was believed due to small amount of inorganic compounds in the rice husk ash left after the heating. When the DTA analyses of the RHA were examined, the reaction was exothermic up to 500 °C and endothermic between 500 - 800 °C. It is thought that the loss of organic component near 800 °C seen in the TGA analysis of RHA increases the porosity since the infiltration process was carried out at the same temperature values.

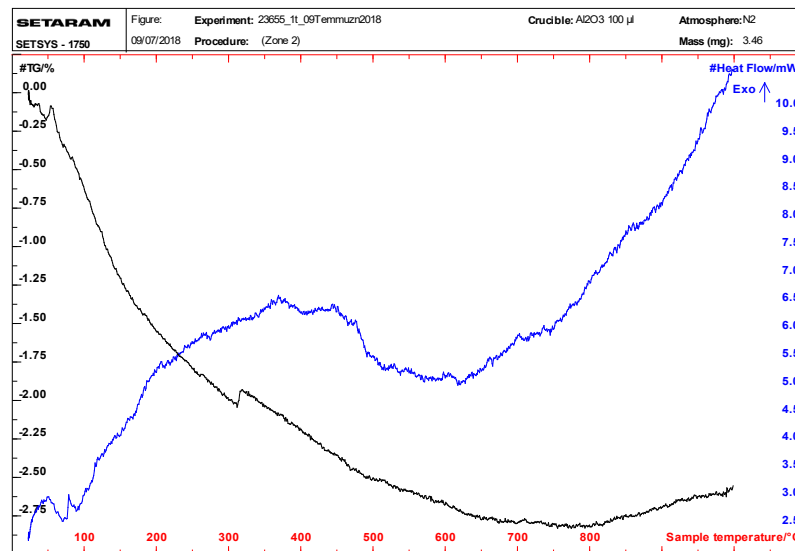


**Figure 7:** TGA-DTA analysis of the RHA reinforcement element

### Hardness Properties

The microstructures were examined for the hardness values of the samples. The hardness values of the samples which are non-aged and aged (T6 heat treated) are shown in Figure 8. It can be seen that the hardness values of the aged samples increased with increasing RHA % volume. However, for samples with T6 heat treatment, only a small increment on hardness was observed for all samples except for non-reinforced sample. This may be explained by the development of  $\text{MgZn}_2$  intermetallic compounds in the matrix and reduction of pores in the non-reinforced sample after heat treatment. The proportional increase in the porosity of the samples and the growth of these pores with heat treatment reduced the hardness of the materials reinforced with RHA. It was found that the sample hardness containing 4 % RHA reinforcement was higher than 1 and 2 % RHA. This can relate of the diffusion of Si from the RHA into the aluminium matrix to form  $\text{SiO}_2$  compound. However, due of the existence of porosity from the RHA, the hardness value is



still lower than the non-reinforced sample after heat treatment. Additionally, promising results were obtained compared to stir casting method which is one of the widespread methods in metal matrix composite production [25].

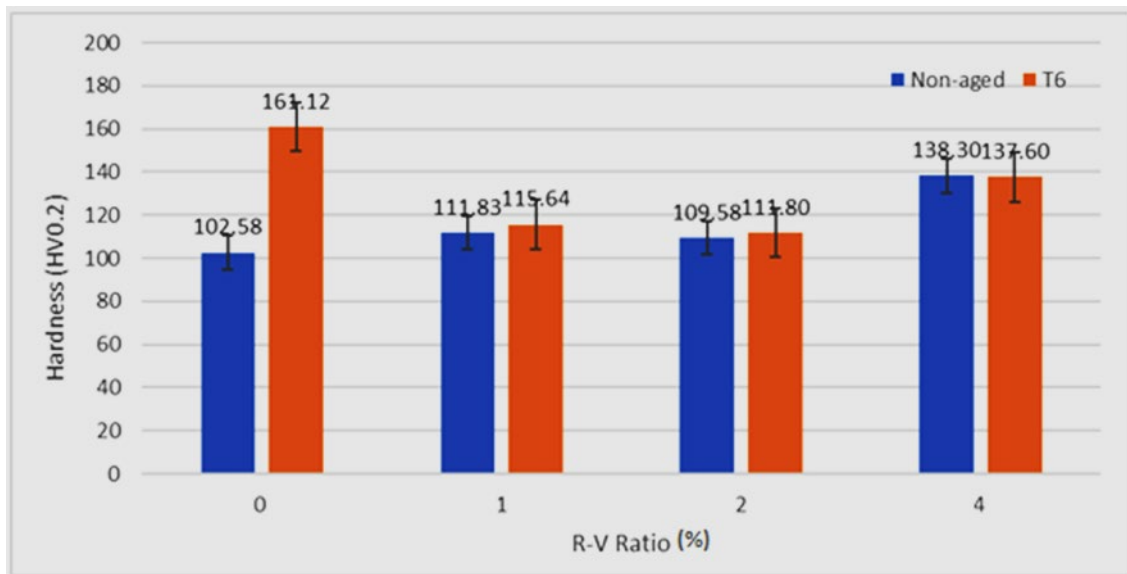


**Figure 8:** Hardness values of as-cast and T6 heat treated samples

### ***Wear Properties***

Figure 9 shows the morphology of the worn surface using SEM analysis for non-reinforced and aluminium composites (AA7075) reinforced with different amounts of RHA. SEM image of the alloy without reinforcement (Figure 9(a)) (depending on the direction of sliding), the plastic deformation in the sample can be clearly seen. Due to the load applied during the wear tests, the plastic flow occurs on the surface of the aluminium composites. Again, in the SEM images given in Figures 9(b) to (d) (on the aluminium composites with 1, 2 and 4 vol.% RHA reinforced), the micro debris detached from the surface of the sample remain in the tribological system and were again adhered to the surface of the composite. The reason for these micro debris was remain in the tribological system is that the structure of these composites has a porous structure. This view is consistent with the result of mass loss values of the composites after wear test as shown in Table 2. As the amount of pore increased, the number of micro debris adhered to the surface of the aluminium composites increased, since these pores act as crack source leading to detrimental effect on wear properties of the composites. Therefore, the debris broken away from the porous surface readily were smeared and embedded in the matrix over the wear test. Similar observation was reported by Gui et al. [26].

**Table 2:** Mass loss values after wear test

RHA R-V (vol%)	0	1	2	4
Before (g)	17.422	21.737	17.544	20.723
After (g)	15.724	19.547	14.818	1.789
Mass Loss (g)	1.6980	2.190	2.726	2.833

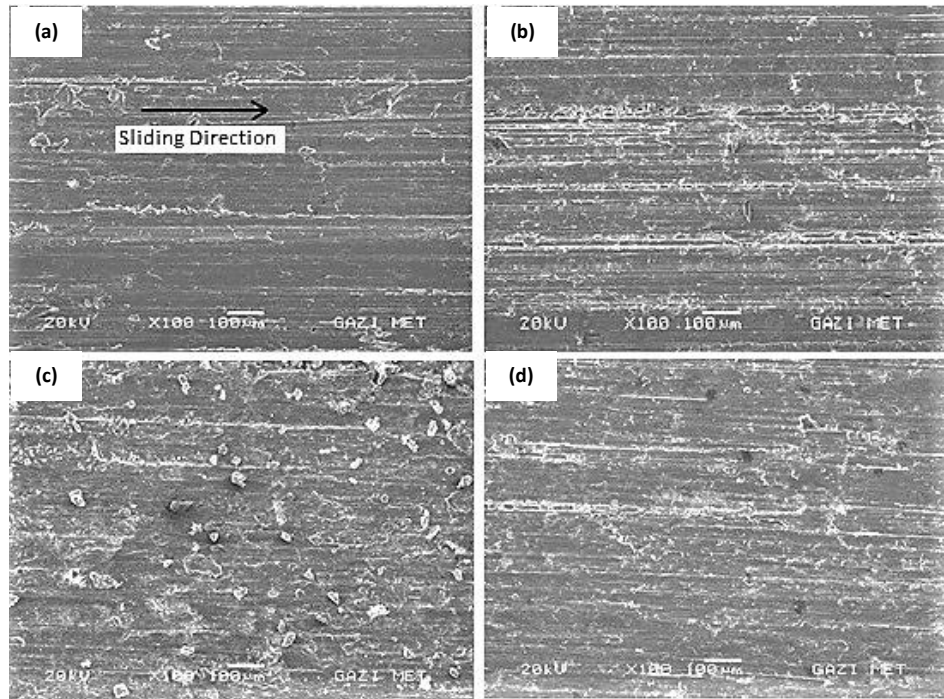


**Figure 9:** Worn surface SEM images of heat-treated samples (a) 0 vol% RHA (non-reinforcement), (b) 1 vol% RHA, (c) 2 vol% RHA and (d) 4 vol% RHA

In addition, these results are similar to previous studies carried out by Özyürek and Tekeli [27]. When the wear surfaces were examined, it was observed that the adhesive wear mechanism is the dominant type of wear in this study with incorporation of RHA into the composite [28].

## Conclusions

For non-aged sample, it was found that the porosity of AMC increased as the RHA reinforcement vol % increased with the highest porosity is 4 vol.% RHA. After T6 heat treatment (aging), the size of pores was expanded due to the expansion of the pores and diffusion of the matrix by the migration effect of Si and O atoms in the grain. From SEM analysis, it was found the  $MgZn_2$  intermetallic compounds were homogeneously formed in T6 heat-treated samples which indicated the aging heat treatment process was successfully applied. The hardness of the non-aged and aged samples increased proportional to the strengthening ratio with the highest hardness value for non-aged sample with 4 vol% RHA. In the T6 heat treated samples, the highest hardness value was found in the unreinforced sample. After examined the worn surfaces, it was seen that the wear consumption was by the adhesive wear mechanism. The mass loss increased with increasing reinforcement vol % and the highest mass loss value was occurred in the sample of 4 vol% RHA. It can be concluded that the vacuum infiltration method has been successfully applied to produce AMC with RHA as reinforcement.

## Acknowledgments

This work was supported by Scientific Research Projects Coordination Unit of Kırıkkale University. Project number 2020/100 and 2017/081.

## Author Contributions

All authors contributed to the data analysis, drafting, and critical revision of the paper, and they all agree to accept responsibility for all aspects of the work.

## Disclosure of Conflict of Interest

The authors have no disclosures to declare.

## Compliance with Ethical Standards

The work is compliant with ethical standards.

## References

- [1] Dursun, T. & Soutis, C. (2014). Recent Developments in Advanced Aircraft Aluminium Alloys. *Materials & Design*, 56, 862-871.
- [2] Liu, J., Zheng, Z., Wang, J., Wu, Y., Tang, W. & Lü, J. (2008). Pressureless Infiltration of Liquid Aluminum Alloy into SiC Preforms to Form Near-net-shape SiC/Al Composites. *Journal of Alloys and Compounds*, 465(1-2), 239-243.
- [3] Aksöz, S., Bican, O., Çalın, R. & Bostan, B. (2014). Effect of T7 Heat Treatment on the Dry Sliding Friction and Wear Properties of the SiC-reinforced AA 2014 Aluminium Matrix Composites Produced by Vacuum Infiltration. *Part J: Journal of Engineering Tribology*, 228(3), 312-319.
- [4] Bahrami, A., Soltani, N., Pech-Canul, M.I. & Gutiérrez, C. A. (2016). Development of Metal-matrix Composites from Industrial/agricultural Waste Materials and Their Derivatives. *Critical Reviews in Environmental Science and Technology*, 46(2), 143-207.
- [5] Chandla, K. N., Kaushik, J. C. & Suri, N. M. (2017). Review on Analysis of Stir Cast Aluminium Metal Matrix Composite from Agro-Industrial Wastes. *i-manager's Journal on Material Science*, 5(2), 35-46.
- [6] Jose, J., Christy, T., Eby, P. P., Feby, J., George, A., Joseph, J., Gautham, C. R. & Benjie, N. (2018). Manufacture and Characterization of A Novel Agro-waste Based Low Cost Metal Matrix Composite (MMC) by Compocasting. *Materials Research Express*, 5, 66035.
- [7] Dele-Afolabi, T.T., Azmah Hanim, M. A., Norkhairunnisa, M., Sobri, S., Calin, R. & Ismarrubie, Z. N. (2018). Significant Effect of Rice Husk and Sugarcane Bagasse Pore

Formers on the Microstructure and Mechanical Properties of Porous Al<sub>2</sub>O<sub>3</sub>/Ni Composites. *Journal of Alloys and Compounds*, 743, 323-331.

[8] Dele-Afolabi, T. T., Hanim, M. A. Azmah., Norkhairunnisa, M., Sobri, S., Calin, R. & Ismarrubie, Z. N. (2018). Tensile Strength and Corrosion Resistance Properties of Porous Al<sub>2</sub>O<sub>3</sub>/Ni Composites Prepared with Rice Husk Pore-forming Agent. *Ceramics International*, 44(10), 11127-11135.

[9] Kumar, A., Mohanta, K., Kumar, D. & Parkash, O. (2012). Properties and Industrial Applications of Rice Husk: A Review. *International Journal of Emerging Technology and Advanced Engineering*, 2, 86-90.

[10] Verma, N. & Vettivel, S. (2018). Characterization and Experimental Analysis of Boron Carbide and Rice Husk Ash Reinforced AA7075 Aluminium Alloy Hybrid Composite. *Journal of Alloys and Compounds*, 741, 981-998.

[11] Mohamad Aznan, M. N., Azmah Hanim, M. A., Suraya, M.T., Norkhairunnisa, M. & Azizan, A. (2017). Properties of Alumina with RHA-reinforced Aluminum Composite Using Different Sintering Profile. *Journal of the Australian Ceramic Society*, 53(1), 187-191.

[12] Ahamed, A. A., Ahmed, R., Hossain, M. B. & Billah, M. M. (2016). Fabrication and Characterization of Aluminium-Rice Husk Ash Composite Prepared by Stir Casting Method. *Rajshahi University Journal of Science and Engineering*, 44, 9-18.

[13] Alaneme, K., Akintunde, I., Olubambi, P. & Adewale, T. (2013). Fabrication Characteristics and Mechanical Behaviour of Rice Husk Ash – Alumina Reinforced Al-Mg-Si Alloy Matrix Hybrid Composites. *Journal of Materials Research and Technology*, 2 (1), 188-194.

[14] Prasad, D. S. (2011). Production and Mechanical Properties of A356.2 /RHA Composites. *International Journal of Advanced Science and Technology*, 33, 51-58.

[15] Prasad, D. S. & Krishna, A. R. (2012). Tribological Properties of A356.2/RHA Composites. *Journal of Materials Science & Technology*, 28(4), 367-372.

[16] Gladston, J., Dinaharan, I., Sheriff, N. & Selvam, J. (2017). Dry Sliding Wear Behavior of AA6061 Aluminum Alloy Composites Reinforced Rice Husk Ash Particulates Produced Using Compocasting. *Journal of Asian Ceramic Societies*, 5(2), 127-135.

[17] Chung, W. S. & Lin, S. J. (1996). Ni-coated SiCp Reinforced Aluminum Composites Processed by Vacuum Infiltration. *Materials Research Bulletin*, 31(12), 1437-1447.

[18] Dong, C. G., Wang, R. C., Chen, Y. X., Wang, X. F., Peng, C. Q. & Jing, Z. E. N. G. (2020). Near-Net Shaped Al/Sicp Composites via Vacuum-Pressure Infiltration Combined with Gelcasting. *Transactions of Nonferrous Metals Society of China*, 30(6), 1452-1462.

[19] Liao, J., Chen, Z., Guan, T., Li, Y., Xiao, Q. & Xue, L. (2021). High Compression Performance of Cf/SiC-Al Composites Fabricated by CVI and Vacuum Pressure Infiltration. *Materials Science and Engineering: A*, 811, 141051.

- [20] Liao, J., Chen, Z., Li, B., Liu, J., Guan, T., Yu, S. & Wang, Y. (2019). Microstructure and Mechanical Properties of Cf/SiC–Al Composites Fabricated by PIP and Vacuum Pressure Infiltration Processes. *Journal of Alloys and Compounds*, 803, 934-941.
- [21] Fu, H., Huang, Y., Wu, H., Yang, Y. & Zong, M. (2016). Synthesis by Vacuum Infiltration, Microstructure, and Thermo-Physical Properties of Graphite–Aluminum Composite. *Advanced Engineering Materials*, 18(9), 1609-1615.
- [22] Calin, R. & Citak, R. (2007). Effect of Powder Size on Infiltration Height in Producing MgO Reinforced Al Matrix Composite by Vacuum Infiltration Method. *Materials Science Forum*, 546, 611-614.
- [23] Zhang, H., Feng, P. & Akhtar, F. (2017). Aluminium Matrix Tungsten Aluminide and Tungsten Reinforced Composites by Solid-State Diffusion Mechanism. *Scientific Reports*, 7(1), 1-8.
- [24] Kumar, R., Bhowmick, H., Gupta, D. & Bansal, S. (2021). Development and Characterization of Multiwalled Carbon Nanotube-Reinforced Microwave Sintered Hybrid Aluminum Metal Matrix Composites: An Experimental Investigation on Mechanical and Tribological Performances. Proceedings of the Institution of Mechanical Engineers. Part L: *Journal of Materials: Design and Applications*, 235(10), 2310–2323.
- [25] Siddharth, D., Mahato, N. & Rao, J. B. (2017). Synthesis & Characterization of RHA (Rice Husk Ash) Particulates Reinforced A7075 Composites. *Journal of Manufacturing Engineering*, 12(2), 55-61.
- [26] Gui, M., Kang, S. B. & Lee, J. M. (2000). Influence of Porosity on Dry Sliding Wear Behavior in Spray Deposited Al–6Cu–Mn/SiCp Composite. *Materials Science and Engineering: A*, 293(1-2), 146-156.
- [27] Özyürek, D. & Tekeli, S. (2010). An Investigation on Wear Resistance of SiC Reinforced Aluminium Composites Produced by Mechanical Alloying Method. *Science and Engineering of Composite Materials*, 17(1), 31-38.
- [28] Özyürek, D., Yıldırım, M. & Çiftçi, İ. (2012). The Tribological Properties of A356-SiC Metal Matrix Composites Fabricated By Thixomoulding Technique. *Science and Engineering of Composite Materials*, 19(4), 351-356.